CrossMark

ORIGINAL

Identification of Impurities in 5-Aminolevulinic Acid by Two-Dimensional Column-Switching Liquid Chromatography Coupled with Linear Ion Trap Mass Spectrometry

Hang Wang[1] · Sijun Xie[1]

Abstract Identification of impurities in 5-aminolevulinic acid (ALA) by mass spectrometry is difficult, because MS-incompatible mobile phases, such as phosphate buffers or ion-pair reagents, need to be used to separate the major component from impurities. In this study, the unknown impurities in ALA have been identified by two-dimensional (2D) column-switching high-performance liquid chromatography (HPLC) coupled with linear ion trap mass spectrometry (LIT MS). The first-dimensional analytical column was a Gemini C18 (150 mm × 4.6 mm, 5 μm) with a non-volatile salt mobile phase at a flow rate of 1.0 mL min^{-1}, and the second-dimensional analytical column was a ZORBAX SB C8 (150 mm × 4.6 mm, 3.5 μm) with a volatile salt mobile phase at a flow rate of 1.0 mL min^{-1}. The detection wavelength was 205 nm. Mass spectra were acquired with an ESI source, in both positive and negative ion modes. Six impurities were identified by their MS^2 and MS^3 fragments, and the mass fragmentation patterns and structural assignments of these impurities were studied. The results obtained by the two-dimensional column-switching method were further compared with those of the conventional one-dimensional normal-phase HPLC–MS using an amide column and an MS-compatible mobile phase for separation. The two-dimensional column-switching method described herein proved to be advantageous in terms of the number of impurities identified. The column-switching and online demineralization technique made the mobile phase conditions compatible with mass spectrometry. Thus, the method solves the problem of incompatibility between non-volatile salt mobile phases and mass spectrometry, making it worthy of popularization and application in impurity identification.

Introduction

5-Aminolevulinic acid (ALA) is the first compound in the porphyrin synthesis pathway, the pathway that leads to heme in mammals and chlorophyll in plants. It is an important intermediate product in the synthesis of hemoglobin [1]. As a gamma-keto acid derivative with a hydrophilic group, ALA and its related impurities are not retained and may co-elute together on a reversed-phase C18 column [2]. To solve these problems, phosphate buffers and ion-pair reagents have been used in the separation of ALA to improve the peak shape on a C18 column [3, 4]. Ion-exchange chromatography has been used for the determination of ALA in plasma and urine [5]. A capillary electrophoretic method has also been developed for the quantification of ALA and two of its degradation products [6, 7]. However, due to non-volatilization and ionization suppression in the above mobile phase, it is necessary to modify the analytes to meet the requirements of the HPLC–MS analysis. A C8 reversed-phase column has also been used for the quantification of ALA and porphobilinogen in physiological fluids using a chemical derivatization

✉ Hang Wang
hangwang@sjtu.edu.cn

[1] Instrumental Analysis Center, Shanghai Jiao Tong University, Dongchuan Road 800, Shanghai 200240, People's Republic of China

method [8]. Hydrophilic interaction liquid chromatography (HILIC)-electrospray ionization/tandem mass spectrometry has been used for the direct and simultaneous determination of 5-aminolevulinic acid and porphobilinogen in urine [9, 10]. However, the identification of impurities in ALA using the conventional one-dimensional (1D)-HPLC–MS is difficult, because the peak area of the major ingredient ALA is high and there is obvious peak tailing, which may suppress and submerge the signals of other impurities.

Online two-dimensional (2D) separation, heart-cutting or column-switching liquid chromatography show a better separation selectivity and resolving power than the conventional HPLC analysis due to the involvement of different separation modes. 2D-HPLC can significantly increase the resolving power and facilitate separations that cannot be achieved by 1D chromatography [11]. The application of 2D-HPLC has extensively been reported for the analysis of biological samples [12–14], proteomics [15, 16], and natural products [17, 18]. We developed an off-line 2D-HPLC MS method for the proteomics analysis in a previous study [19]. The use of 2D-HPLC in pharmaceutical analysis has also been attracting more attention recently [20–25]. For the pharmaceutical and proteomics analysis, MS-incompatible mobile phases can be used in the first dimension of liquid chromatography, and then, MS-compatible mobile phases can be used in the second dimension [16, 26, 27].

In this study, two-dimensional column switching and online demineralization combined with linear ion trap mass spectrometry have been developed for the identification of unknown impurities in ALA. The column-switching and online demineralization techniques allow the use of conditions that are compatible with mass spectrometry. Six ALA-related impurities were identified by their MS^n fragments, and the mass fragmentation patterns were also studied. In addition, comparative studies employing a conventional one-dimensional normal-phase HPLC–MS method are presented.

Experimental

Chemicals and Reagents

A sample of ALA was provided by Shanghai Fudan-Zhangjiang Bio Pharmaceutical (Shanghai, China). The deionized water used in this study was from a Milli-Q water purification system (Millipore Corp., Bedford, MA, USA). LC–MS grade acetonitrile was purchased from Anpel Laboratory Technologies (Shanghai, China); sodium octanesulfonate (chromatographic grade) was purchased from TCI Chemical Co. (Tokyo, Japan). Potassium dihydrogenphosphate, sodium hydroxide, and hydrochloric acid

were purchased from Shanghai Chemical Reagent Corp. (Shanghai, China). ALA standard was purchased from Alfa Aesar (Lancaster, UK).

Preparation of the Test Solutions

A stock solution of ALA standard or sample was prepared by dissolving 50 mg in 5 mL water. The stock solution was stored at 4 °C in the dark before use. For the one-dimensional normal-phase HPLC–MS analysis, ALA was prepared by dissolving 10 mg in 5 mL water/acetonitrile (50:50).

Alkali Decomposition Test

An aliquot (5 mL) of stock solution was diluted with 5 mL of 0.2 mol L^{-1} sodium hydroxide solution and the mixture was heated in a water bath at 40 °C for 30 min. It was then cooled to room temperature and adjusted to pH 7.0 using 0.2 mol L^{-1} hydrochloric acid. The resulting solution was then diluted to 25 mL with the mobile phase used for the first dimension of chromatography prior to injection.

Heating Decomposition Test

An aliquot (5 mL) of stock solution was heated in a water bath at 85 °C for 2 h. The solution was then cooled to room temperature and diluted to 25 mL with the mobile phase used for the first dimension of chromatography prior to injection.

Instrumentation

Figure 1 shows the set-up of the 2D HPLC system and illustrates the valve configuration. The first dimension includes a ternary pump, an autosampler, a thermostatted column compartment, and a UV detector. The second dimension includes a binary pump, an autosampler, and a thermostatted column compartment with a six-column-switching feature, a diode-array detector, and a linear ion trap mass spectrometer. The interface between the first and second dimensions is a six-loop valve trapping system with a trap column (C18, 12.5 mm × 4.6 mm, 5 μm) connected to a loop ring with a volume of 100 μL from Agilent Technologies (Santa Clara, CA, USA). The two gradient pumps, autosamplers, thermostatted column compartments, UV detector, and diode-array detector are Infinity 1260 HPLC set-ups (Agilent Technologies) with an LTQ XL mass spectrometer equipped with an electrospray ionization (ESI) source (Thermo Fisher Scientific, San Jose, CA, USA). Data acquisition, handling, and instrument control were performed using the Xcalibur 2.3.1 software.

Fig. 1 Scheme for the valve configuration: **a** eluate from the trap column was transferred to analytical column 2 in the second dimension; **b** MS-incompatible mobile phase from analytical column 1 in the first dimension was retained on the trap column
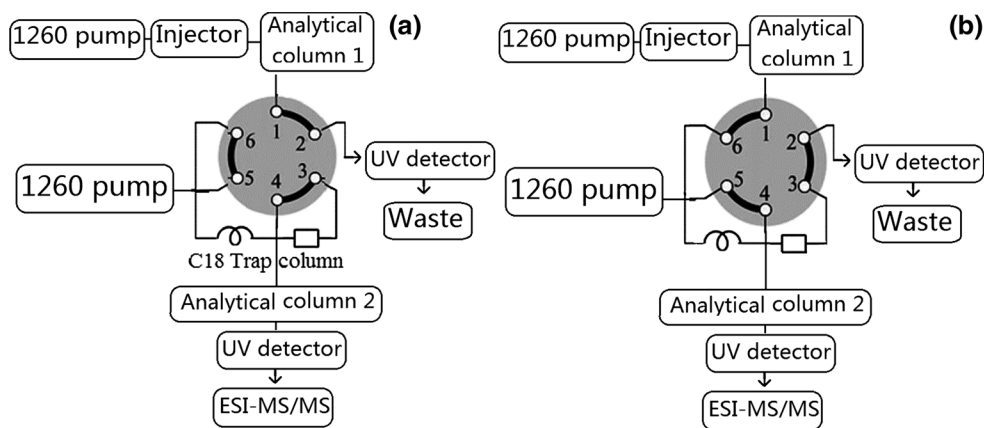
Chromatographic Conditions

The first dimension utilized a Gemini C18 column (150 mm × 4.6 mm, 5 µm; Phenomenex, Torrance, CA, USA) at a temperature of 35 °C. The mobile phase was sodium octanesulfonate (4 mM)/potassium dihydrogenphosphate (pH 2.0; 40 mM)/acetonitrile (43:43:14, *v/v/v*); the flow rate was set to 1 mL min^{-1}, wavelength 205 nm, injection volume 20 µL. The second dimension of chromatography was as follows: ZORBAX SB C8 column (150 mm × 4.6 mm, 3.5 µm; Agilent Technologies); column temperature maintained at 35 °C. Mobile phase A: water (0.1 % acetic acid); mobile phase B: acetonitrile; mobile phase B was set at 3 % in 5 min. The flow rate was set at 1.0 mL min^{-1}, with a split-flow ratio of 1:4 of mass spectrometer to waste. UV detection was performed at 205 nm. The divert times for trapping and elution are listed in Table 1. For comparison, different kinds of columns were investigated, including a Waters Cortecs C18 column® (100 mm × 2.1 mm, 2.7 µm), an Agilent ZORBAX SB C8 column (150 mm × 4.6 mm, 3.5 µm), a Waters Acquity UPLC® HSS T3 column (50 mm × 2.1 mm, 1.8 µm), a Waters XBridge® amide column (150 mm × 2.1 mm, 3.5 µm), and a Thermo Acclaim™ Trinity™ Q1 column (50 mm × 2.1 mm, 3 µm).

Mass Spectrometric Conditions

ESI source, mass range: *m/z* 50 to 1500. In positive mode, the source voltage was 4 kV, the capillary temperature was 350 °C, the sheath gas flow was 40 arbitrary units (arb), the sweep gas flow was 1.0 arb, and the capillary voltage was 24 V. In the MS^2 and MS^3 analyses, the fragmentation was performed through collision-induced dissociation (CID) at collision energies in the range 25–40 eV. In negative mode, the source voltage was 3.5 kV, the capillary temperature was 350 °C, the sheath gas flow was 35 arb, the auxiliary gas flow was 15.0 arb, the sweep gas flow was 1.0 arb, and

the capillary voltage was 43 V. The eluate from the second dimension was diverted to waste for 1 min through a divert valve on the inlet of mass spectrometer. Mass spectrometric scanning was then performed when the divert valve on the inlet of MS was switched from waste to load.

Comparison with One-Dimensional Normal-Phase HPLC–MS Method using an Amide Column

A Waters XBridge® amide column (150 mm × 2.1 mm, 3.5 µm) was used. Mobile phase A was water (20 mM ammonium acetate) and mobile phase B was acetonitrile, with gradient elution: 0–7 min 95 % B–60 % B, 7–19 min 60 % B; the flow rate was 0.25 mL min^{-1}, wavelength 205 nm, injection volume 20 µL. The eluate from 10.5 to 14 min was diverted to waste. In this way, the contamination of the MS source by the major ingredient could be avoided.

Results and Discussion

First-Dimensional HPLC–UV Analysis of ALA with an MS-Incompatible Mobile Phase

As mentioned above, ALA is a gamma-keto acid derivative with a hydrophilic group. Hence, the retention times of ALA or other impurities are short (within 1 min), and such substances may co-elute together using a reversed-phase C18 column. Band broadening and peak tailing were observed using normal-phase amide or HILIC columns, despite the addition of MS-compatible salts, such as 20 mM ammonium acetate or 20 mM ammonium formate. Thus, the above methods using an MS-compatible buffer are not suitable for the separation of the major ingredient and other impurities. In our experiments, an ion-pair reagent was used for separation. Sodium octanesulfonate (4 mM)/potassium dihydrogenphosphate (pH 2.0; 40 mM)/acetonitrile

Table 1 Information on the identified compounds

Peak No.	t_R (1st D)	t_R (2nd D)	Divert time for trap	Divert time for elution	Positive mode (m/z)	Negative mode (m/z)	Chemical name	MS^b (+)	MS^b (+)	Peak area (%)	Chemical structure
1	1.5	1.8	1.0	1.7	114.0	ND^a	Piperidine-2,5-dione (PD)	86.0	ND^b	4.24	
2	1.9	1.5	1.4	2.1	225.1	223.1	2,5-dicarboxy-ethylpyrazine (PY)	207.1, 197.1	179.0, 165.0, 161.1	0.433	
3	2.0	1.2	1.5	2.2	217.1	ND^a	5-amino-4-((4-hydroxy-2-oxobutyl)imino) pentanoic acid (PA)	199.0, 154.9	182.1, 171.0, 155.0	4.50	
4	2.9	1.8	2.4	3.1	132.0	130.0	ALA	113.9	85.9	78.1	
5	4.0	1.8	3.5	4.2	227.1	225.2	2,5-dicarboxyethyl-3, 6-dihydropyrazine (DHPY)	209.0, 191.0, 149.0	191.0, 149.0	8.50	
6	4.6	1.8	4.1	4.8	ND^c	165.0, 201.0	Phthalic acid	137.0, 121.0	93.0	2.94	
7	7.2	2.1	6.7	7.4	245.1	243.2	ALA-dimer	227.1, 209.1	209,1, 191.0, 149.0	0.98	

^{a} Not detected in negative mode

^{b} Not detected at the collision energy of 45 eV

^{c} Not detected in positive mode

Fig. 2 First-dimensional HPLC–UV chromatogram using MS-incompatible buffer (the chromatogram has been enlarged): **a** alkali decomposition test; **b** heating decomposition test
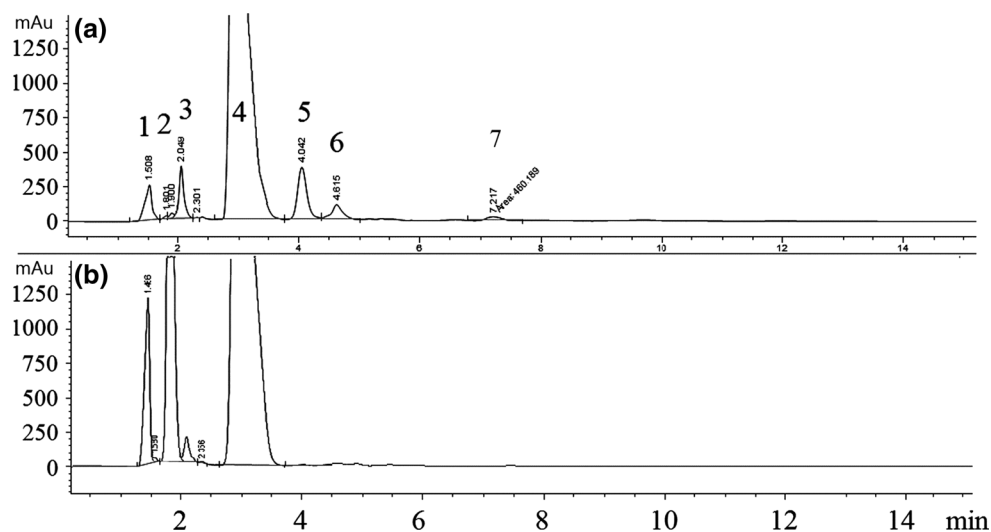
(43:43:14, v/v/v) was used as the mobile phase in the first dimension of HPLC separation. Figure 2a and b show the chromatograms of the ALA sample following alkali decomposition and heating decomposition tests, respectively. As shown in Fig. 2a, six impurities were observed under the alkali decomposition conditions; the peak area

percentages of these impurities compared with the total area of the chromatogram are listed in Table 1; the peak area percentages ranged from 0.433 to 8.50 %. The mobile phase produced good chromatographic peak shapes and resolved all analytes.

Optimization of the Second Dimension of the HPLC Separation Method

Two different trap columns, namely a ZORBAX C18 column (12.5 mm × 4.6 mm, 5 μm) and a C18 column (12.5 mm × 2.1 mm, 5 μm) were compared. The 4.6 mm ID column had an internal volume of about 200 μL, and the 2.1 mm ID column had an internal volume of less than 40 μL. A loop ring with a volume of 100 μL was also connected to the trap column. The flow rate in the first dimension was 1 mL min^{-1}. However, the peak width in the first dimension was 0.3 min, and hence, the 2.1 mm ID column was unable to trap all of the eluate. The 4.6 mm ID column with an internal volume of about 200 μL was sufficient to trap all of the eluate at 0.2 min after the retention time of the corresponding peak observed in the first dimension. A loop ring with a volume of 300 μL without a trap column was also used, but peak broadening was obvious in the second dimension with peak width >1 min. The 4.6 mm ID column could trap and enrich the fraction from the first dimension, and decrease the peak broadening in the second dimension with a peak width <0.5 min.

The choice of column for the second dimension is important for desalting and separation of impurities from the MS-incompatible mobile phase. Different kinds of columns were investigated in our preliminary experiments, including a Waters Cortecs C18 column® (100 mm × 2.1 mm, 2.7 μm), an Agilent ZORBAX SB C8 column (150 mm × 4.6 mm, 3.5 μm), a Waters Acquity UPLC® HSS T3 column (50 mm × 2.1 mm, 1.8 μm), a Waters XBridge® amide column (150 mm × 2.1 mm, 3.5 μm), and a Thermo Acclaim™ Trinity™ Q1 column (50 mm × 2.1 mm, 3 μm). The total ion chromatograms (TICs) of the second-dimensional system with different columns are shown in the Supplementary Material Figs. S1–S3. Impurities were eluted within 1 min using a C18 column even with a high ratio of phase A to phase B (water/acetonitrile, 98:2) at a flow rate of 0.25 mL min^{-1}. A T3 column was used with 100 % water, but the impurities were also eluted within 1 min at a flow rate of 0.15 mL min^{-1}; thus, not all of the impurities could be separated from potassium dihydrogenphosphate and sodium octanesulfonate. For the HPLC separation of ALA with the Waters Cortecs C18 column, the Agilent ZORBAX SB C8 column, and the Waters T3 column by the conventional 1D method using a mobile phase of water/acetonitrile (97:3), ALA was eluted at 1.4 min, 1.6 min, and 1.2 min, respectively. When a small amount of mobile phase

eluted from the first dimension, that is, 300 μL of sodium octanesulfonate (4 mM)/potassium dihydrogen phosphate (pH 2.0; 40 mM)/acetonitrile (43:43:14, *v/v/v*), the composition of the mobile phase in the second dimension changed greatly. The retention times of ALA on the C18 and T3 columns decreased to 0.7 min, but its retention time on the C8 column increased to 1.8 min. The small amount of mobile phase A eluted from the first dimension may have slightly increased the retention of ALA on the C8 column. Gong-Xin He also found that the retention times of strongly polar compounds with amino and carboxyl acid groups, such as L-carnitine and crotonoylbetaine, increased on a C8 column when using sodium octanesulfonate as a mobile phase, whereas their retention times decreased on a C18 column [28].

An amide column was further used under the gradient elution conditions. The retention times of analytes were sensitive to the mobile phase in amide column separation; a small increase in water content in the mobile phase shortened the retention times of the target compounds. For the HPLC separation of ALA and related impurities on an amide column by the conventional 1D method, samples were prepared in water/acetonitrile (50:50), and the injection volume was small at only 20 μL; thus, the composition of mobile phase did not change greatly. However, when the small amount of mobile phase eluted from the first dimension was sodium octanesulfonate (4 mM)/potassium dihydrogenphosphate (pH 2.0; 40 mM)/acetonitrile (43:43:14, *v/v/v*), the aqueous phase constituted 86 % thereof, and the volume of the interface between the first and second dimensions was 300 μL; thus, the composition of the mobile phase in the second dimension changed greatly. The increase of water content in the mobile phase greatly shortened the retention times of impurities on the amide column, such that all of the impurities eluted within 1 min. Dihydrogenphosphate and ion-pair reagents could be used to suppress the signals of target impurities. An Acclaim Trinity Q1 column was used under the gradient elution conditions, but the target impurities co-eluted with MS-incompatible buffer at 2.6 min and could not be separated. Thus, in our experiments, a C8 column was used for the analysis of the target compounds. All of the impurities were eluted after 1.2 min, while potassium dihydrogenphosphate eluted within 1 min, thus permitting their separation. The MS-incompatible salts were diverted to waste for 1 min through a divert valve on the inlet of mass spectrometer.

Second Dimension of HPLC–MS/MS Identification of Impurities in ALA with an MS-Compatible Mobile Phase

To reduce fluctuation of the baseline in the first dimension and to increase the compatibility of the organic phase

Fig. 3 Synthesis route and the possible by-products of ALA
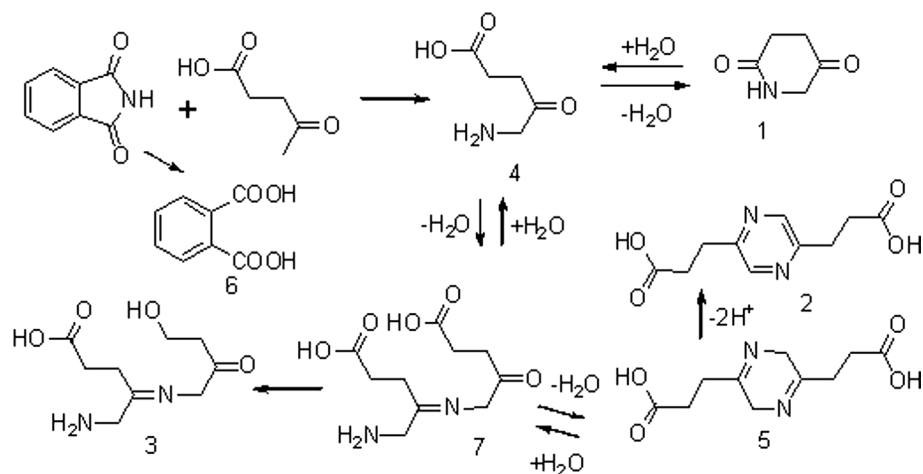
between the two different dimensions, acetonitrile was used as organic phase in the second dimension. To identify the structures of impurities, six impurities and the main component from the first dimension were trapped individually for each injection and transferred to the analytical column in the second dimension, as shown in Fig. 1a and b. In the second dimension of the HPLC-LIT MS analysis, the valve was set at the position of Fig. 1b at 0.5 min before the retention time of the corresponding peaks in the first dimension, then switched from the position in Fig. 1b to that in Fig. 1a at 0.2 min after the retention time of the corresponding peak observed in the first dimension (which means the time delay between divert time for trap and divert time for elution is 0.7 min). After 1 min, the valve was switched to the original position (Fig. 1b) and the first-dimensional column was eluted with the mobile phase for the next injection. When the second dimension separation was carried out, the first separation was not stopped and was eluted, thus other peaks of impurities were waste for every injection in the first dimension. In our experiment, the elution time in the second dimension was 5 min for one cycle of analysis of impurities, and this elution time was longer than the time interval between those peaks in the first dimension; thus, samples had to be injected into the 1D-HPLC system several times to identify all of the impurities.

The analytes in the trap column were eluted to the second-dimensional C8 analytical column and finally eluted to the ESI–MS/MS system. To remove the remaining ion-pair reagents and phosphate salts eluted from trap column, the eluate from the C8 analytical column was diverted to waste for 1 min to avoid elution of the salts to the mass spectrometer. In this way, ion suppression caused by non-volatilized salts was significantly reduced. MS signals in both positive and negative modes were obtained for these impurities and structures were elucidated on the basis of MS^n information. According to the literature, ALA can be synthesized from 4-oxopentanoic acid and phthalimide [3]. 2-aminoacetic acid is also involved as a reactant in the biosynthesis method [29]. Under the alkaline conditions, the formation of 2,5-dicarboxyethyl-3,6-dihydropyrazine (DHPY), porphobilinogen, and pseudoporphobilinogen via an open-chain dimeric ketimine has previously been postulated, and the oxidation of DHPY to 2,5-dicarboxy-ethylpyrazine (PY) in the presence of oxygen has also been reported [6, 30]. The synthesis route and the possible by-products are shown in Fig. 3. The retention times of each peak in the first and second dimensions, m/z in positive and negative modes, MS^2 and MS^3 fragments, chemical names, divert times, and the structures are listed in Table 1. The impurities were identified as the degradation products, the dimer product, the dehydration product, the oxidative product, and the hydrolysis product from the reactant.

Peak 1 was assigned to piperidine-2,5-dione (PD) with $[M + H]^+$ at m/z 114.0; the TIC and EIC of peak 1 in the second dimension are shown in Fig. 4. No fragment ion was generated with collision energy of 30 eV due to the structure of the lactam ring. A further increase in collision energy from 30 to 40 eV generated product ions at m/z 86.0 (the MS^1 and MS^2 spectra are given in Supplementary Material Figs. S4 and S5). The product ion was attributed to cleavage of a carbonyl group, which led to loss of a molecule of CO.

Peak 2 was assigned to 2,5-dicarboxy-ethylpyrazine (PY) with $[M + H]^+$ at m/z 225.1. Figure 5 shows the TIC and EIC of peak 2 in the second dimension. The main dissociation processes are the loss of one molecule of either H_2O or CO from the precursor ion at m/z 225.1, which generate the peaks at m/z 207.1 and 197.1, respectively. The MS^3 product ions from that at m/z 207.1 include those at m/z 179.0, 165.0, and 161.1, which are generated from the further loss of CO, CH_2CO, and H_2O, respectively (the MS^1, MS^2, and MS^3 spectra are shown in Supplementary Material Figs. S6–S8).
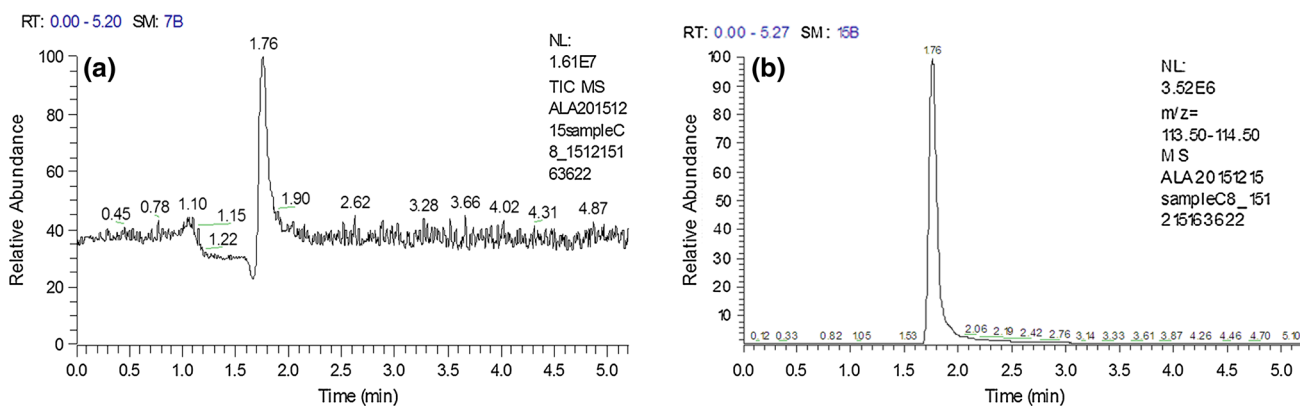
Fig. 4 TIC and EIC of peak 1 in the second dimension: **a** TIC, **b** EIC, m/z 114.0
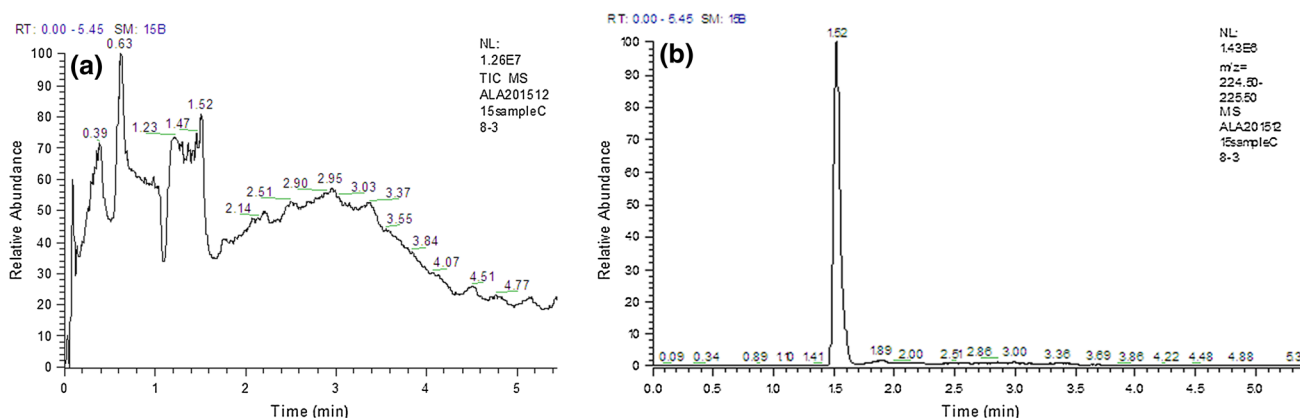

Fig. 5 TIC and EIC of peak 2 in the second dimension: **a** TIC, **b** EIC, m/z 225.1
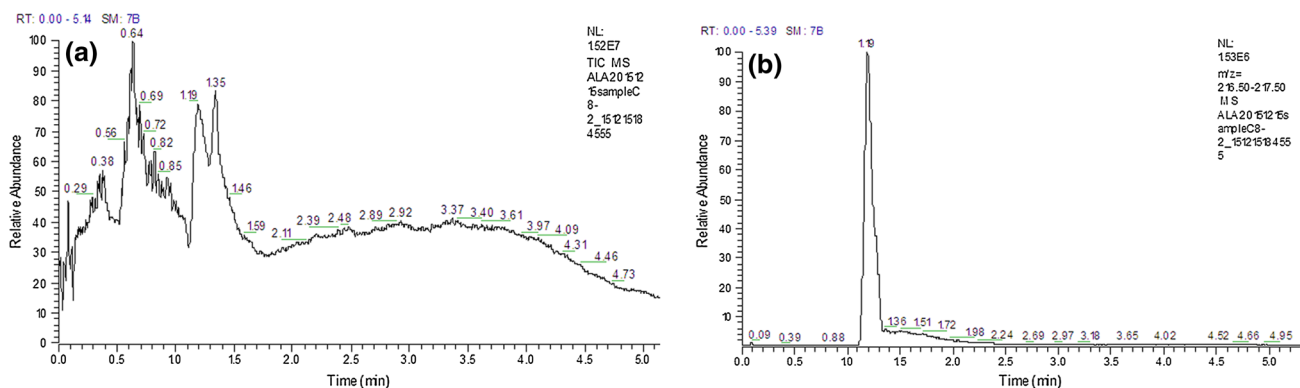

Fig. 6 TIC and EIC of peak 3 in the second dimension: **a** TIC, **b** EIC, m/z 217.1

Peak 3 was identified as 5-amino-4-[(4-hydroxy-2-oxobutyl)imino]pentanoic acid (PA) with $[M + H]^+$ at m/z 217.1. Figure 6 shows the TIC and EIC of peak 3 in the second dimension. The MS^1, MS^2, and MS^3 spectra of peak 3 are shown in Supplementary Material Figs. S9–S11. The main dissociation process is the loss of a molecule of water from the precursor ion at m/z 217.1, which generates the peak at m/z 199.0. That at m/z 154.9 is generated by the loss of CO_2 from a carboxyl group. The MS^3 product ions from that at m/z 199.0 include those at m/z 182.1, 171.0,

and 155.0, which are generated by loss of NH_3, CO, and CO_2, respectively.

Peak 4 is the major component ALA with $[M + H]^+$ at m/z 132.0 (MS^1 spectrum shown in Supplementary Material Fig. S12). The main dissociation process is the loss of a molecule of water, which generates the peak at m/z 113.9 (shown in Supplementary Material Fig. S13). The MS^3 product ion at m/z 85.9 was produced from the MS^2 product ion at m/z 113.9 (the MS^3 spectrum is given in Supplementary Material Fig. S14).

Peak 5 was assigned to 2,5-dicarboxyethyl-3,6-dihydro-pyrazine (DHPY) with $[M + H]^+$ at m/z 227.1 (see Supplementary Material Fig. S15). The main dissociation process is the breakage of an αC-βC bond and the loss of one and two molecules of water from the precursor ion at m/z 227.1, which generates the peaks at m/z 149.0, 209.0, and 191.0, respectively (the MS^2 spectrum is shown in Supplementary Material Fig. S16). The peaks at m/z 191.0 and m/z 149.0 were also produced from the MS^2 product ion at m/z 209.0 in the MS^3 spectrum (the MS^3 spectrum is given in Supplementary Material Fig. S17).

Peak 6 was detected as $[M - H]^-$ at m/z 165.0 and $[M + Cl]^-$ at m/z 201.0 in negative mode; m/z 137.0 and 121.0 were observed in the MS/MS spectrum, which were produced by loss of a molecule of CO or CO_2, respectively, from the precursor ion at m/z 165.0. Peak 6 was identified as phthalic acid, produced by the hydrolysis of phthalimide (the MS^1 and MS^2 spectra are shown in Supplementary Material Figs. S18 and S19).

Peak 7 was identified as ALA dimer with $[M + H]^+$ at m/z 245.1 (see Supplementary Material Fig. S20). The main dissociation process is the loss of one molecule of water from the precursor ion at m/z 245.1, which generates the peak of DHPY at m/z 227.1 (see Supplementary Material Fig. S21). The main dissociation process from m/z 227.1 is the same as the MS^2 fragmentation of DHPY, which generates MS^3 product ions at m/z 209.1, 191.0, and 149.0 (the MS^3 spectra are shown in Supplementary Material Fig. S22).

In the heating decomposition test, the peak at 1.9 min increased in the HPLC–UV chromatogram of the first dimension (see Fig. 2b). This peak was trapped and transferred to the second-dimensional column; m/z 225.1 was also observed for this peak in the MS^1 spectrum. The MS^1 and MS^2 spectra are consistent with peak 2 in Table 1 and thus attributable to PY.

Validation of the 2D Column-Switching HPLC-LIT MS Method

Analytical characteristics, including repeatability, linearity, and LOD were investigated. For the establishment of a linearity equation, different concentrations of ALA standards (50, 10, 5, 2.5, 1, 0.5, and 0.2 µg mL^{-1}) were prepared. The EIC with m/z 132.0 was used for peak integration. Linear regression plots were obtained by plotting the peak area of the target standards versus the theoretical concentrations. Good linearity was obtained for the ALA standards in the range from 0.2 to 50 µg mL^{-1}, with a correlation coefficient >0.99. To check the reproducibility of the developed method, a repeatability study was performed at three different concentration levels. Three replicate experiments were carried out for each concentration level with 0.5, 1, and 5 µg mL^{-1} of ALA. The repeatabilities, expressed as the relative standard deviation (RSD), were within 9.1 %. The LOD of the method was estimated based on the analysis of ALA standard at S/N of three times the average of the baseline. The ALA standard was diluted to different concentrations and the EIC with m/z 132.0 was obtained. The LOD was 100 ng mL^{-1}. The results showed that the proposed analytical method is reliable.

Comparison with the One-Dimensional Normal-Phase HPLC–MS Method using an Amide Column

One-dimensional normal-phase HPLC–MS using an amide column was also performed for comparison with the two-dimensional column-switching HPLC–ESI–MS/MS method developed in our study; the MS-compatible mobile phase was used. The HPLC–UV chromatogram using an amide column is shown in the Supplementary Material Fig. S23. Three impurities, namely PA, PY, and DHPY, were identified for the ALA sample following the alkali decomposition test, with retention times of 2.2, 4.9, and 7.2 min, respectively. The peak of the main component at 11.0 min showed a significant broadening and tailing, with peak width >5 min; other impurity peaks may have been submerged in the main peak and such materials could have been simultaneously diverted to waste. Drifting baselines in chromatography also affect the veracity of analysis due to the gradient conditions and the UV cut-off absorption of the solvent at 205 nm. Thus, the two-dimensional column-switching method developed in this study is advantageous in terms of the number of impurities identified compared with one-dimensional normal-phase HPLC–MS using an amide column.

Conclusions

We have developed a new analytical method with column-switching HPLC-ESI-MS^n for the identification of six impurities in ALA. The chemical structures of these impurities have been identified using MS-incompatible mobile phases in the first dimension and MS-compatible mobile phases in the second dimension. The column-switching

and online demineralization technique made the chromatographic conditions for ALA determination compatible with mass spectrometry. The use of this column-switching technology led to a significant increase in the number of identified impurities compared with the conventional normal-phase HPLC–MS using an amide column. The developed method is expected to prove very useful for solving the problem of incompatibility between a non-volatile salt mobile phase and mass spectrometry in impurity identification.

Compliance with Ethical Standards

Conflict of interest All authors declare that they have no conflict of interest.

Ethical approval This article does not contain any studies with human participants or animals performed by any of the authors.

References

1. Benton CM, Lim CK, Moniz C, Jones DJL (2012) Travelling wave ion mobility mass spectrometry of 5-aminolaevulinic acid, porphobilinogen and porphyrins. Rapid Commun Mass Spectrom 26:480–486

2. Alsarra IA, Eldeen A, Yassin B, Abdel-Hamid M, Alanazi FK, Aljuffali IA (2011) Direct UPLC–MS–MS validated method for the quantification of 5-aminolevulinic acid: application to in vitro assessment of colonic-targeted oral tablets. J Chromatogr Sci 49:428–433

3. He CC, Guan J, Ding S, Yan F, Shi S, Niu QL (2013) Determination of 5-aminolevulinic acid and related four substances by reversed-phase ion-pair high-performance liquid chromatography. J. Shenyang Pharm Univ 9:696–700

4. Chen ZK, Peng XS, Wu W (2007) Study on determination of aminolevulinic acid and its related substances by RP-HPLC. Chin Pharm J 421:1895–1897

5. Floderus Y, Sardh E, Moller C, Andersson C, Rejkjaer L, Andersson DEH, Harper P (2006) Variations in porphobilinogen and 5-aminolevulinic acid concentrations in plasma and urine from asymptomatic carriers of the acute intermittent porphyria gene with increased porphyrin precursor excretion. Clin Chem 52:701–707

6. Bunke A, Zerbe O, Schmid H, Burmeister G, Merkle HP, Gander B (2000) Degradation mechanism and stability of 5-aminolevulinic acid. J Pharm Sci 891:1335–1341

7. Lord GA, Luo JL, Lim CK (2000) Capillary zone electrophoresis/mass spectrometry of 5-aminolaevulinic acid and porphobilinogen. Rapid Commun Mass Spectrom 14:314–316

8. Zhang JL, Yasuda M, Desnick RJ, Balwani M, Bishop D, Yu CL (2011) A LC-MS/MS method for the specific, sensitive, and simultaneous quantification of 5-aminolevulinic acid and porphobilinogen. J Chromatogr B 879:2389–2396

9. Benton CM, Couchman L, Marsden JT, Rees DC, Moniz C, Lim CK (2013) Direct and simultaneous quantitation of 5-aminolaevulinic acid and porphobilinogen in human serum or plasma by hydrophilic interaction liquid chromatography-atmospheric pressure chemical ionization/tandem mass spectrometry. Biomed Chromatogr 27:267–272

10. Benton CM, Couchman L, Marsden JT, Rees DC, Moniz C, Lim CK (2012) Direct and simultaneous determination of 5-aminolaevulinic acid and porphobilinogen in urine by hydrophilic interaction liquid chromatography-electrospray ionisation/tandem mass spectrometry. Biomed Chromatogr 26:1033–1040

11. Ren Q, Wu C, Zhang J (2013) Use of on-line stop-flow heart-cutting two-dimensional high-performance liquid chromatography for simultaneous determination of major constituents in tartary buckwheat (*Fagopyrum tataricum Gaertn*). J Chromatogr A 1304:257–262

12. Park M, Kim J, Park Y, In S, Kim E, Park Y (2014) Quantitative determination of 11-nor-9-carboxy-tetrahydrocannabinol in hair by column switching LC–ESI-MS[3]. J Chromatogr B 947–948:179–185

13. Neubauer W, Kig A, Bolekc R, Trittler R, Engelhardt M, Jung M, Kummerer K (2009) Determination of the antifungal agent posaconazole in human serum by HPLC with parallel column-switching technique. J Chromatogr B 877:2493–2498

14. Hu L, Boos KS, Ye M, Zou H (2014) Analysis of the endogenous human serum peptides by on-line extraction with restricted-access material and HPLC-MS/MS identification. Talanta 127:191–195

15. Essader AS, Cargile BJ, Bundy JL, Stephenson JL Jr (2005) A comparison of immobilized pH gradient isoelectric focusing and strong-cation-exchange chromatography as a first dimension in shotgun proteomics. Proteomics 5:24–34

16. Delmotte N, Lasaosa M, Tholey A, Heinzle E, Huber CG (2007) Two-dimensional reversed-phase x ion-pair reversed-phase HPLC: an alternative approach to high-resolution peptide separation for shotgun proteome analysis. J Proteome Res 6(11):4363–4373

17. Wang D, Chen LJ, Liu JL, Wang XY, Wu YL, Fang MJ, Wu Z, Qiu YK (2015) On-line two-dimensional countercurrent chromatography × high performance liquid chromatography system with a novel fragmentary dilution and turbulent mixing interface for preparation of coumarins from *Cnidium monnieri*. J Chromatogr A 1406:215–223

18. Stoll DR (2010) Recent progress in online, comprehensive two-dimensional high-performance liquid chromatography for non-proteomic applications. Anal Bioanal Chem 397:979–986

19. Wang H, Sun SN, Zhang Y, Chen S, Liu P, Liu B (2015) An off-line high pH reversed-phase fractionation and nano-liquid chromatography–mass spectrometry method for global proteomic profiling of cell lines. J Chromatogr B 974:90–95

20. Venkatramani CJ, Wigman L, Mistry K, Chetwyn N (2012) Simultaneous, sequential quantitative achiral–chiral analysis by two-dimensional liquid chromatography. J Sep Sci 35:1748–1754

21. Venkatramani CJ, Al-Sayah M, Li G, Goel M, Girotti J, Zang L, Wigman L, Yehl P, Chetwyn N (2016) Simultaneous achiral-chiral analysis of pharmaceutical compounds using two-dimensional reversed-phase liquid chromatography-supercritical fluid chromatography. Talanta 148:548–555

22. Li J, Xu L, Shi ZG, Hu M (2015) A novel two-dimensional liquid chromatographic system for the online toxicity prediction of pharmaceuticals and related substances. J Hazard Mater 293:15–20

23. Sheldon EM (2003) Development of a LC–LC–MS complete heart-cut approach for the characterization of pharmaceutical compounds using standard instrumentation. J Pharm Biomed Anal 31:1153–1166

24. Huidobro AL, Pruim P, Schoenmakers P, Barbas C (2008) Ultra rapid liquid chromatography as second dimension in a

comprehensive two-dimensional method for the screening of pharmaceutical samples in stability and stress studies. J Chromatogr A 1190:182–190

25. Alexander AJ, Ma LJ (2009) Comprehensive two-dimensional liquid chromatography separations of pharmaceutical samples using dual Fused-Core columns in the 2nd dimension. J Chromatogr A 1216:1338–1345

26. Zhang J, Lanham KA, Heideman W, Peterson RE, Li L (2013) Characterization of zebrafish cardiac proteome using online pH gradient SCX-RP HPLC-MS/MS platform. Methods Mol Biol 1005:119–127

27. Zhang K, Li Y, Tsang M, Chetwyn NP (2013) Analysis of pharmaceutical impurities using multi-heartcutting 2D LC coupled with UV-charged aerosol MS detection. J Sep Sci 36:2986–2992

28. He GX, Dahl T (2000) Improved high-performance liquid chromatographic method for analysis of L-carnitine in pharmaceutical formulations. J Pharm Biomed Anal 15:315–321

29. Yamamoto T (2015) Method for microbial manufacture of 5-aminolevulinic acid or salt thereof. Jpn. Kokai Tokkyo Koho, 2015181459 (22) JP 2015181459

30. McCarron PA, Donnelly RF, Andrews GP, Woolfson AD (2005) Stability of 5-aminolevulinic acid in novel non-aqueous gel and patch-type systems intended for topical application. J Pharm Sci 94:1756–1771